

Conference on Nuclear Isospin, Asilomar-Pacific Grove, 1969, edited by J. D. Anderson, S. D. Bloom, J. Cerny, and W. True (Academic Press Inc., New York, 1969).

¹⁵N. Cue and P. Richard, *Phys. Rev.* **173**, 1108 (1968).

¹⁶L. S. Michelman and C. F. Moore, *Phys. Letters* **26**, 446 (1968).

¹⁷A. I. Yavin, R. A. Hoffswell, L. H. Jones, and T. M. Noweir, *Phys. Rev. Letters* **16**, 1049 (1966).

¹⁸R. G. Clarkson, Technical Report No. 3, Center for Nuclear Studies, University of Texas (unpublished).

¹⁹R. G. Clarkson and C. E. Watson, unpublished.

²⁰J. K. Dickens, E. Eicher, R. J. Silva, and G. Chilosi, Oak Ridge National Laboratory Report No. ORNL-3934 (unpublished).

²¹F. D. Becchetti, Jr., and G. W. Greenlees, *Phys. Rev.*

182, 1190 (1969).

²²P. J. A. Buttle and L. J. B. Goldfarb, *Proc. Phys. Soc. (London)* **83**, 701 (1964).

²³B. L. Cohen and O. V. Chubinsky, *Phys. Rev.* **131**, 2184 (1963).

²⁴G. Clausnitzer, G. Graw, C. F. Moore, and K. Wienhard, *Phys. Rev. Letters* **22**, 793 (1969).

²⁵R. A. Hinrichs, G. W. Phillips, J. G. Cramer, and H. Wieman, *Bull. Am. Phys. Soc.* **14**, 121 (1969).

²⁶P. Richard, private communication.

²⁷L. S. Michelman and C. F. Moore, unpublished.

²⁸J. K. Dickens and E. Eicher, *Nucl. Phys.* **101**, 408 (1967).

²⁹R. G. Clarkson and W. R. Coker, following paper [*Phys. Rev. C* **2**, 1108 (1970)].

Charge Exchange in $^{92}\text{Zr}(d,p)^{93}\text{Zr}^\dagger$

R. G. Clarkson* and W. R. Coker

Center for Nuclear Studies, The University of Texas, Austin, Texas 78712

(Received 30 July 1969; revised manuscript received 11 June 1970)

Excitation functions for the $^{92}\text{Zr}(d,p)^{93}\text{Zr}$ reaction to eight low-lying states in ^{93}Zr were measured from 4.2- to 11.2-MeV incident deuteron energy, a region including the (d,n) thresholds to the analogs of the observed states. Charge-exchange effects were observed for at least the $d_{5/2}$ ground state in ^{93}Zr . Also, $^{92}\text{Zr}(d,d)$ angular distributions were taken at 6.25, 7.5, and 11.0 MeV, in 5° steps from 40 to 165° , in order to obtain deuteron optical parameters. A $^{92}\text{Zr}(p,p)$ angular distribution was taken at 10.75-MeV proton energy in order to obtain proton optical parameters. Orbital angular momenta and estimates of spectroscopic factors were obtained for three previously unreported states in ^{93}Zr . The results of distorted-wave Born-approximation calculations for the excitation curves are discussed.

1. INTRODUCTION

A cusplike behavior exhibited in (d,p) excitation functions for several nuclei, almost all in the mass-90 region, has been the subject of several recent experimental investigations.¹⁻⁶ Such behavior is always observed near the threshold for the (d,n) reaction to the isobaric analog of the final state observed in the (d,p) reaction, and has been attributed to charge-exchange coupling.⁷⁻⁹ In particular, $^{90}\text{Zr}(d,p)$ has been extensively studied^{1,2}; also, to a lesser extent, (d,p) reactions on ^{91}Zr , ^{92}Zr , and ^{94}Zr have been studied.^{1,2,4-6} Results of some of these investigations are discussed in Ref. 1.

In this article, we report on a study of $^{92}\text{Zr}(d,p)^{93}\text{Zr}$, including optical-model analysis of elastic scattering at appropriate energies in deuteron and proton channels, excitation functions for all observed states, and a complete distorted-wave Born-approximation (DWBA) analysis. Figure 1 shows a level diagram of the observed states in ^{93}Zr and their analogs in ^{93}Nb . The present work is a continuation and extension of the earlier investigations,

with the aim of making a thorough experimental study of the charge-exchange effect for a particular case and providing information regarding the isotopic systematics of the effect.

2. EXPERIMENTAL METHOD

The deuteron and proton beams for this experiment were obtained from the 12-MeV model-EN tandem Van de Graaff accelerator at the Center for Nuclear Studies, University of Texas at Austin. A beam of approximately $0.3 \mu\text{A}$ on target was used during most of the experiment. The beam energy spread was estimated to be less than 4 keV. Deuteron beams of energies from 4 to 11 MeV, and a proton beam of 10.75 MeV, were used. The beam energy was controlled by a 90° analyzing magnet, with the usual nuclear-magnetic-resonance probe. The magnet was calibrated using the $^{27}\text{Al}(p,n)$ threshold at 5.803 MeV.

The ^{92}Zr target was a rolled self-supporting foil, purchased from Oak Ridge National Laboratory, Separated Isotope Division, and enriched to 94.6% ^{92}Zr . The target isotopic thickness was determined

from low-energy, forward-angle, elastic proton and deuteron scattering. Measurements were made at several angles and energies, to insure that the observed cross sections were due solely to Coulomb scattering. Various detectors were used to minimize systematic errors from measurements of detector solid angle; results obtained from different detectors agree to within 7%. The ^{92}Zr -target isotopic thickness was determined as 0.46 mg/cm².

The excitation-function data were accumulated with two 3-mm-thick Si(Li) detectors placed at lab angles of 168 and 138° with respect to the incident beam, angles chosen because the charge-exchange effect has been observed primarily at backward angles.¹⁻⁵ Collimators were mounted in front of each detector to define the solid angle and to decrease background from slit scattering. The detectors were cooled to -78°C in order to improve their resolution. In addition, permanent magnets were mounted before each detector to prevent electrons emitted by the target from entering the detector.

A Digital Equipment Corporation PDP-7 computer was used on-line for data storage and analysis, with 1024 channels provided for each detector. An integrated beam of 200 μC was collected for each data point. The experimental resolution was determined to be 40–50 keV. Preliminary analyses of the spectra, as well as continuous data monitoring, was carried out automatically by the program SUPERVISOR,¹⁰ which also wrote the data on standard IBM magnetic tapes. Final analysis was carried out from the tapes on the University of Texas CDC 6600 computer, using the program DRAFT,¹¹ which performed a least-squares fit of Gaussian peaks on a polynomial background to the desired region of each spectrum. An example

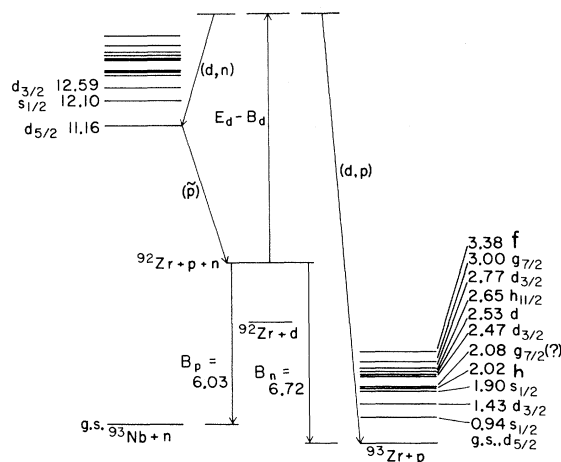


FIG. 1. Schematic energy-level diagram for $^{92}\text{Zr}(d, p)^{93}\text{Zr}$ and analogous $^{92}\text{Zr}(d, n)^{93}\text{Nb}^A$ reactions.

of such a fit for a typical spectrum is shown in Fig. 2.

3. RESULTS AND ANALYSIS

A. Elastic Scattering Angular Distribution

Deuteron elastic scattering angular distributions were taken at 6.25-, 7.5-MeV, and 11.0-MeV incident deuteron energy, and a proton elastic scattering angular distribution was taken at 10.75 MeV, in order to perform optical-model analyses. The angular distributions were taken in 5° steps from 40 to 165° (plus 168°) at each energy. These deuteron and proton angular distributions are shown in Fig. 3. Also shown in Fig. 3 is the $^{92}\text{Zr}(p, p)$ angular distribution at 12.7 MeV from data taken by Dickens *et al.*¹²

Optical-model fits to the deuteron elastic scattering data were obtained using a program written by Smith,¹³ as modified by P. A. Moore and the authors. In order to eliminate ambiguities in the fits, we required that the optical parameters fit the data at 6.25, 7.5, and 11.0 MeV simultaneously, allowing only a linear dependence of real and imaginary well depths on energy. In preliminary analysis, reasonable fits were obtained for all deuteron elastic scattering data using several sets of deuteron optical parameters for ^{92}Zr . Two sets of deuteron parameters were obtained, referred to as Sets A and B. Set A was obtained by starting the search with the ^{90}Zr potential of Dally, Nelson, and Smith.¹⁴ Set B was obtained starting with the Perey and Perey¹⁵ averaged parameters. The parameter Sets A and B are given in Table I. The χ^2 values for Sets A and B were obtained assuming a fractional error of $\pm 10\%$ for all data points. The calculated deuteron elastic scattering angular distributions are shown with the data in Fig. 3(a).

The proton elastic angular distribution at 10.75 MeV and the 12.7-MeV angular distribution of Dickens *et al.*¹² were similarly fitted using an opti-

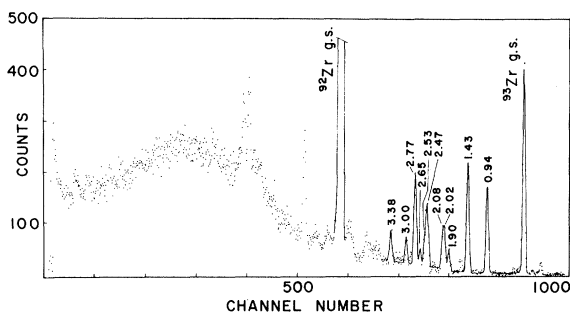


FIG. 2. Energy spectrum of charged particles from $^{92}\text{Zr} + d$ at 11.0 MeV, observed at a lab angle of 105°. Superimposed on the high-energy end of the spectrum are peak fits generated by the program DRAFT.

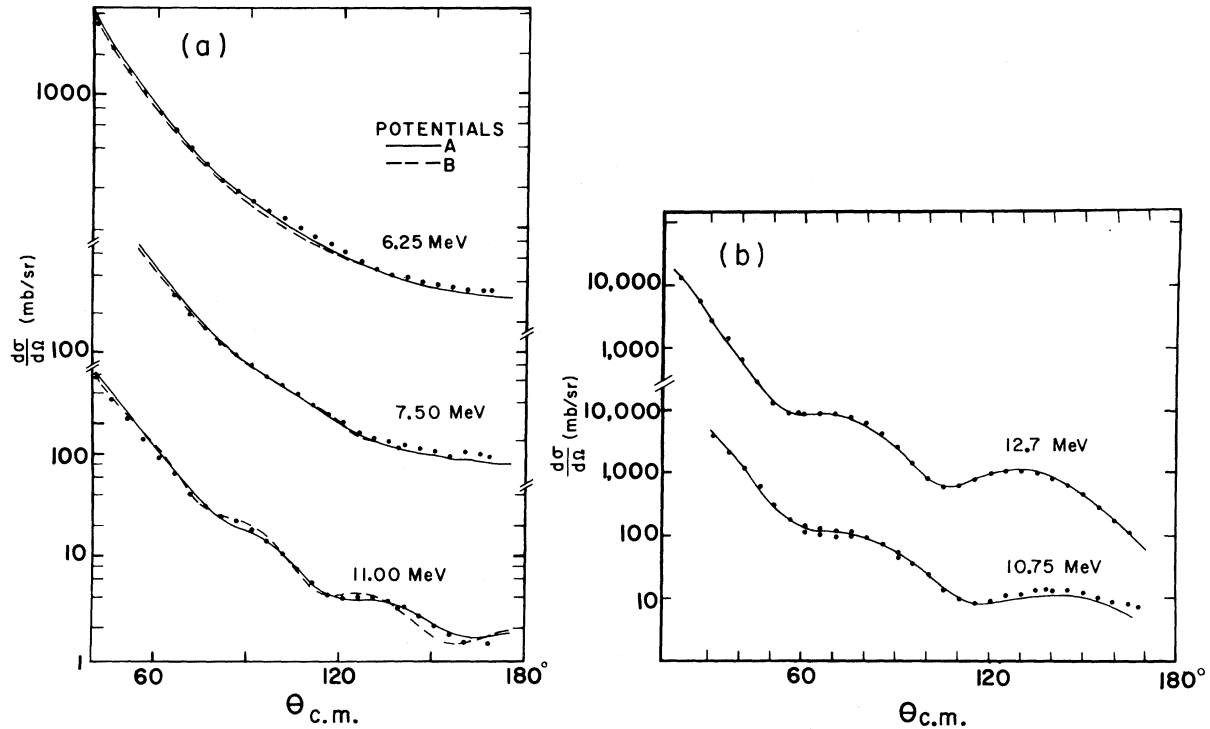


FIG. 3. (a) Deuteron elastic scattering angular distributions for ^{92}Zr target at 6.25, 7.50, and 11.0 MeV. The solid and dashed curved are, respectively, optical-model fits with parameter Sets A and B (see Table I). (b) Proton elastic scattering angular distributions for ^{92}Zr target at 12.7 and 10.75 MeV. The 12.7-MeV data is that of Dickens *et al.* (Ref. 12). Optical-model Set E is used (see Table II).

cal-model program written by Perey. Three sets of proton potentials, referred to as D, E, and F, were obtained. Set D was obtained by starting with the potential of Dickens, Eichler, and Satchler.¹² Set E was obtained starting with Set D, except for substituting spin-orbit parameters determined from $^{92}\text{Zr}(p,p)$ polarization measurements of Kossanyi-Demay and de Swiniarski.¹⁶ These two sets gave identical fits, and only Set E is given in Table II. Set F in Table II was obtained by starting with the average parameters of Perey,¹⁷ again with modified spin-orbit parameters. The χ^2 values for the various potentials were obtained assuming a fractional error of 5% for the 10.75-MeV data, and with the quoted errors given by

Dickens *et al.*¹² for the 12.7-MeV data. The calculated proton elastic scattering angular distributions are shown with the data in Fig. 3(b).

B. Excitation Functions

Excitation functions were obtained for (d,p) reactions to the ground state ($d_{5/2}$), and to the 0.94-MeV ($s_{1/2}$), 1.43-MeV ($d_{3/2}$), 1.90-MeV ($s_{1/2}$), 2.47-MeV ($d_{3/2}$), 2.77-MeV ($d_{3/2}$), 3.00-MeV ($g_{7/2}$), and 3.38-MeV ($l \geq 2$) states in ^{93}Zr .¹⁸ The measurements were made for incident deuteron energies from 4.2 to 6.0 MeV in 100-keV steps, and from 6.0 to 11.2 MeV in 50-keV steps. This energy region encompasses the threshold energies for the

TABLE I. Survey of optical parameters for $^{92}\text{Zr}(d,d)^{92}\text{Zr}$.

E_{lab} (MeV)	V (MeV)	r_0 (fm)	a_0 (fm)	W_D (MeV)	r' (fm)	a' (fm)	V_{so} (MeV)	r'' (fm)	a'' (fm)	r_C (fm)	Ref.
6.25	88.61	1.278	0.72	15.85	1.29	0.747	0.0	1.278	a, Set A
	99.0	1.15	0.61	5.48	1.68	0.849	4.78	1.15	0.61	1.15	a, Set B
7.5	87.08	1.278	0.72	15.85	1.29	0.747	0.0	1.278	a, Set A
11.0	82.77	1.272	0.72	15.85	1.29	0.747	0.0	1.278	a, Set A
15.0	90.0	1.23	0.64	12.0	1.18	0.93	0.0	1.30	18

^aThis work.

TABLE II. Survey of optical parameters for $^{92}\text{Zr}(p, p)^{92}\text{Zr}$.

E_{lab} (MeV)	V (MeV)	r_0 (fm)	a_0 (fm)	W_D (MeV)	r' (fm)	a' (fm)	V_{s_0} (MeV)	r'' (fm)	a'' (fm)	r_C (fm)	Ref.
10.75	55.34	1.23	0.60	9.66	1.18	0.67	6.4	1.20	0.42	1.25	a, Set E
12.7	52.2	1.25	0.65	12.3	1.25	0.525	6.0	1.25	0.65	1.25	12
	55.08	1.23	0.60	9.66	1.18	0.67	6.4	1.20	0.42	1.25	a, Set E
	53.1	1.23	0.64	10.0	1.23	0.76	7.0	1.23	0.64	1.25	b
	52.6	1.25	0.65	13.5	1.25	0.47	6.75	1.20	0.42	1.25	a, Set F
	54.5	1.23	0.596	9.2	1.18	0.668	6.4	1.23	0.596	1.23	12
14.25	50.0	1.25	0.65	9.0	1.25	0.65	6.2	1.25	0.65	1.25	c
18.6	51.49	1.24	0.65	12.27	1.28	0.50	6.78	1.20	0.42	1.25	16
19.4	50.9	1.20	0.70	10.3	1.25	0.65	6.2	1.20	0.70	1.25	d
22.5	46.6	1.26	0.66	10.6 ^e	1.23	0.567	7.72	1.26	0.664	1.26	f

^aThis work.^bJ. K. Dickens and E. Eichler, Nucl. Phys. **101**, 408 (1967).^cK. Matsuda *et al.*, J. Phys. Soc. Japan, **22**, 1311 (1967).^dM. M. Stautberg and J. J. Kraushaar, Phys. Rev. **151**, 969 (1966).^e $W=0.5$ MeV, also.^fJ. B. Ball, C. B. Fulmer, and R. H. Bassel, Phys. Rev. **135**, B706 (1964).

(d, n) reactions to the analogs in ^{93}Nb of all the states considered in ^{93}Zr . Specifically, the threshold energies range from 7.38-MeV incident deuteron energy for the analog of the ^{93}Zr ground state to 10.8 MeV for the analog of the 3.38-MeV state.

As previously discussed, the excitation-function data were taken at 138 and 168° in order to be sure of observing any threshold effects which might be present. Deuteron elastic scattering excitation curves were also obtained at these angles. These elastic scattering curves were well represented by optical-model calculations using either parameter Set A or B, and exhibit no resonant structure from 4.2 to 11.2 MeV.

As shown in Fig. 4, the excitation curves for the $d_{5/2}$ ground state indeed exhibit a strong threshold effect near 7.38-MeV deuteron energy. The 168°

curve confirms the results of Heffner *et al.*⁵ and is similar to results found for other Zr isotopes.^{1,2,4} As expected,¹ the effect is very important at 168° and is markedly reduced at 138°. The various curves in Fig. 4 are results of DWBA calculations, as discussed in Sec. 4 of this paper. The DWBA calculations are rather insensitive to the particular proton parameter set used, as can be seen in Fig. 4 for potentials AD, AE, and AF. However, the calculations are rather sensitive to the deuteron potential.

The measured cross sections for the (d, p) reactions to the $s_{1/2}$ states at 0.94 and 1.90 MeV are shown in Fig. 5. The thresholds for the (d, n) reactions to the corresponding analog states are 8.32 and 9.3 MeV, respectively. The measured cross section does differ noticeably from the prediction of approximate finite-range DWBA calculations near the charge-exchange threshold, particularly for the lower-lying $s_{1/2}$ state, but the over-all trend of the curves is well described. These results tend to confirm observations^{1,3,5} that the charge-exchange effect diminishes with increasing (d, n) threshold energy, vanishing when $Q < \frac{1}{4}\Delta_C$, where Q is the (d, p) Q value and Δ_C the Coulomb displacement energy of a proton in the residual nucleus.⁹

The excitation curves for $d_{3/2}$ states at 1.43-, 2.47-, and 2.77-MeV excitation energy are shown in Fig. 6. The corresponding (d, n) analog-state thresholds are 8.8, 9.8, and 10.1 MeV, respectively. The data are generally fitted quite well by the DWBA calculations shown. However, in all three cases, the 138° DWBA calculations tend to give a good description of the cross section below the respective thresholds, while the measured cross sections in all three cases decrease to a lower value than the DWBA prediction as the deuteron

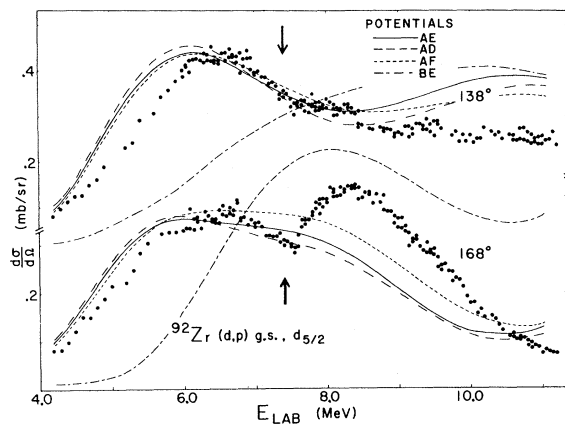


FIG. 4. Excitation curves for $^{92}\text{Zr}(d, p)^{93}\text{Zr}(d_{5/2}, \text{g.s.})$ at 138 and 168°, from 4 to 11 MeV. The curves are zero-range DWBA calculations using the deuteron potentials A and B, and the proton potentials D, E, and F (see Tables I and II).

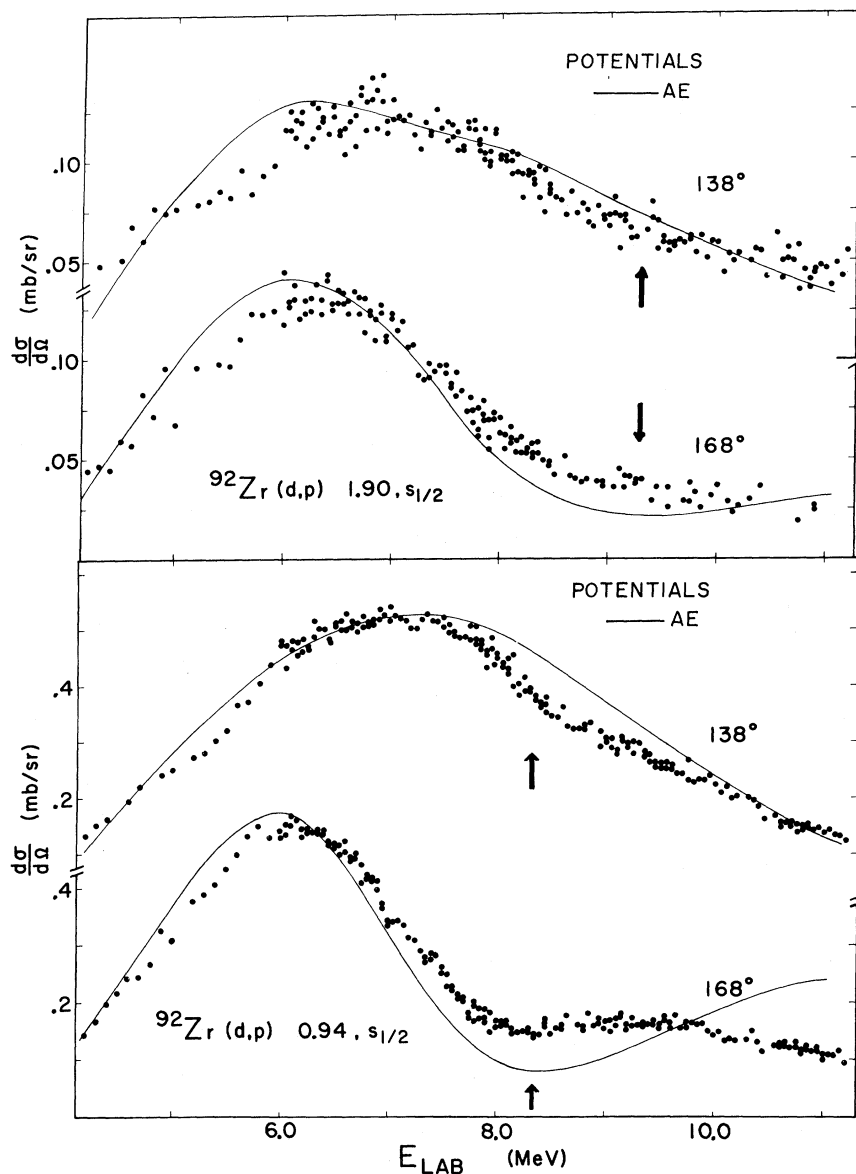


FIG. 5. Excitation curves for $^{92}\text{Zr}(d,p)^{93}\text{Zr}(s_{1/2})$, 0.94 MeV and $s_{1/2}$, 1.90 MeV at 138° and 168° , from 4 to 11 MeV. The solid curves are local-energy-approximation DWBA calculations using potentials A and E (see Tables I and II).

energy increases beyond threshold. Such discrepancies can hardly be attributed *a priori* to charge-exchange threshold effects. Coupled-channel DWBA calculations⁹ for an $l=2$ transition in $^{90}\text{Zr}(d,p)$, with $Q < \frac{1}{4}\Delta_C$, indicate that at 155° the manifestation of the charge-exchange coupling can indeed be a slight depression of the cross section just above threshold (see Fig. 5 of Ref. 9). However, the fact that here 168° is always well fitted, and the 138° fit is consistently "off" in all three cases, makes an explanation due to charge exchange unlikely.

Excitation curves were also obtained for the states at 3.00 MeV ($g_{7/2}$) and 3.38 MeV ($l \geq 2$). The data extend only slightly above the charge-exchange

threshold for these two states, but the measured cross sections are fitted rather well by the DWBA calculations, as shown in Fig. 7.

C. Spectroscopy of ^{93}Zr

Nuclear spectroscopy was not the purpose of this experiment, but a number of states of ^{93}Zr were observed, including three previously unreported. A brief discussion of these results will therefore be given. Angular distributions extending from 50° to 170° at 5° intervals were accumulated at 6.25, 7.5, and 11.0 MeV for the eight low-lying states for which excitation curves are shown in Figs. 4–7, as well as states at 2.02, 2.08, 2.53, and 2.65 MeV (see Table III). The levels at 2.02

and 2.08 MeV were observed by Cohen and Chubinsky¹⁸ as an unresolved doublet, which our data resolves at most angles. The same situation holds for the 2.47- and 2.53-MeV states. Forward-angle data would, of course, be preferred for reliable extraction of spectroscopic factors and l values, but we are able to make tentative assignments for both. Results are summarized in Table III. We assign $l=5$ to the 2.02- and 2.65-MeV states, confirm Ref. 18's assignment of $l=4$ for the 2.08-MeV state, and assign $l=2$ to both 2.47- and 2.53-MeV states. Also, we find $l \geq 2$ for the state at 3.38

MeV in contrast to Ref. 18's $l=1$ assignment. Work published after submission of this manuscript confirms several of those assignments. Booth *et al.*¹⁹ confirm $l=5$ for the 2.02-MeV state, while Kent, Lieb, and Moore,²⁰ find $l=3$ for the isobaric analog of the 3.38-MeV state.

4. DISCUSSION

The DWBA (d, p) excitation-function calculations shown in Figs. 4 through 7 were done with a program, modified by one of us (W.R.C.), based on the DWBA codes NEPTUNE and VENUS, written by Tamura, Rybicki, and Coker.²¹ The calculations were done including spin-orbit coupling, in the zero-range approximation, except for the $s_{1/2}$ transitions. The $s_{1/2}$ transition calculations were done with a version of the program which includes a finite-range approximation.²²

The DWBA calculations were used to obtain l values and "normalization" factors for the twelve states observed in ^{93}Zr up to 3.5-MeV excitation energy. The results of these calculations and a comparison with the results of Cohen and Chubinsky¹⁸ are given in Table III. The values given are

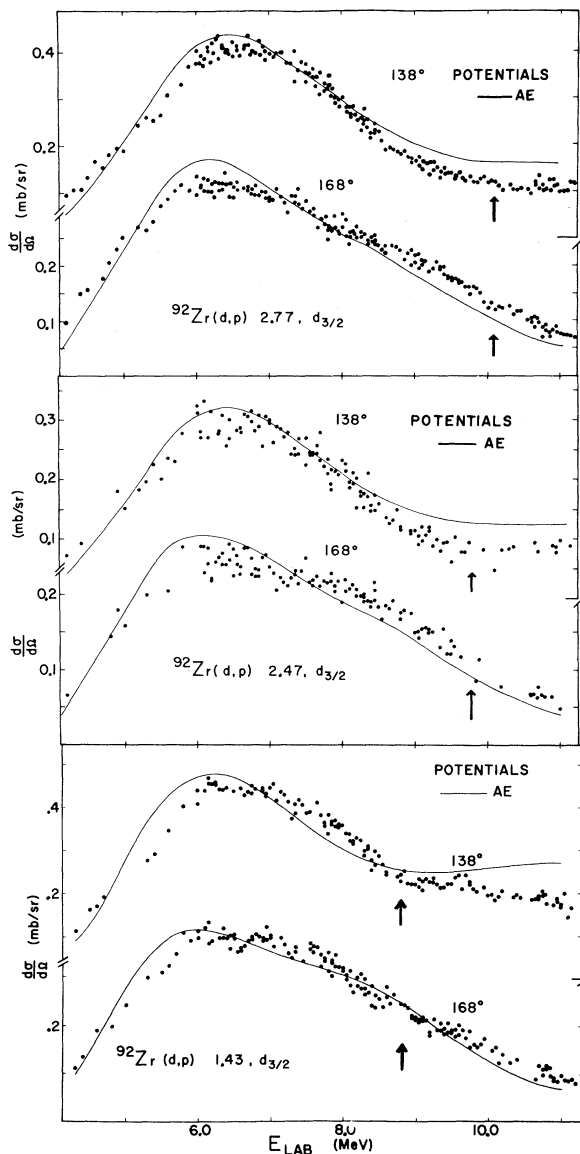


FIG. 6. Excitation curves for $^{92}\text{Zr}(d, p)^{93}\text{Zr}(d_{3/2})$ states at 1.43, 2.47, and 2.77 MeV at 138 and 168°, from 4 to 11 MeV. The solid curves are zero-range DWBA calculations using potentials A and E (see Tables I and II).

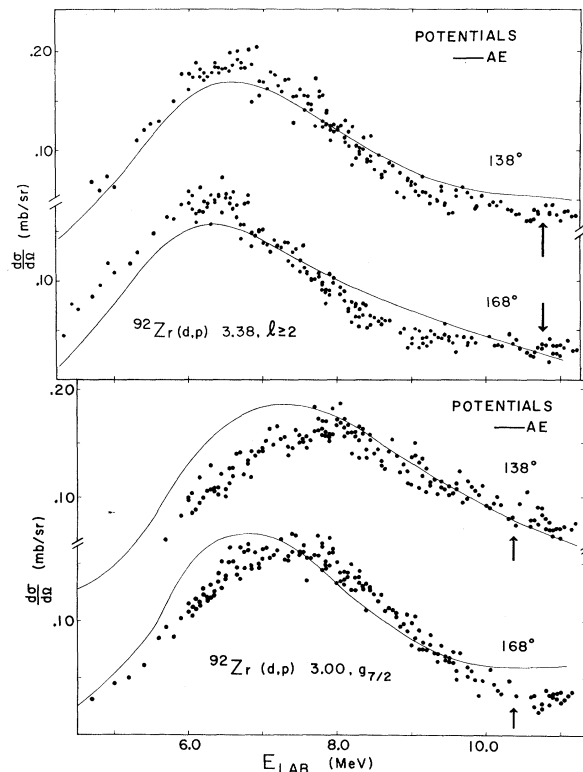


FIG. 7. Excitation curves for $^{92}\text{Zr}(d, p)^{93}\text{Zr}(g_{7/2})$ at 3.00 MeV, $d-f$ at 3.38 MeV at 138 and 168°, from 4 to 11 MeV. The solid curves are local-energy-approximation DWBA calculations using potentials A and E (see Tables I and II).

TABLE III. Energy levels in ^{93}Zr , with spectroscopic factors from the DWBA analyses of Ref. 18. Values in parentheses are uncertain. "Normalization" factors used in this work are given for comparison; l_j values are those assigned in this work.

Excitation (MeV)	l_j	S_{lj} This work	S_{lj} Ref. 18
0.0	$d_{5/2}$	0.55	0.54
0.28
0.94	$s_{1/2}$	0.70	0.91
1.43	$d_{3/2}$	0.60	0.38
1.64	$g_{7/2}$...	0.11
1.90	$s_{1/2}$	0.13	0.21
2.02 ^a	(h)	0.20	...
2.08	($g_{7/2}$)	0.48	0.42
2.32	($g_{7/2}$)	...	0.09
2.47	($d_{3/2}$)	0.25	0.24
2.53 ^a	(d)	0.08	...
2.65 ^a	$h_{11/2}$	0.12	...
2.77	(d)	0.29	0.21
3.00	$g_{7/2}$	0.37	0.30
3.19	($d_{3/2}$)	...	0.38
3.29	($d_{3/2}$)	...	0.03
3.38	($f-d$)	~ 0.10	0.12 ^b

^aNot reported in Ref. 18.

^b S_{lj} calculated assuming $p_{3/2}$ state.

averages for the three energies at which each angular distribution was taken, 6.25, 7.5, and 11.0 MeV.

The DWBA calculations of the available excitation functions, shown in Figs. 4 through 7 and discussed in the previous section, were done using the "normalization" factors of Table III. Except for the charge-exchange threshold effects previously discussed, the DWBA calculations are seen to provide quite good fits to these excitation functions over the broad energy range measured here. The quality of the fits is particularly gratifying considering the fact that the data are at angles 138 and 168°, well within the region frequently not

quantitatively fitted by DWBA calculations.

Reports²³ exist of an anomaly in the $^{90}\text{Zr}(d, p)$ ($d_{5/2}$, g.s.) spectroscopic factor at the (d, n) threshold. While the study here cannot rule out such behavior, since we do not include the forward stripping peaks in our data, it does seem clear that charge exchange can have very little, if any, effect on the total (d, p) cross section. Therefore we feel that one should not be concerned about the possibility of charge-exchange effects leading unknown experiments to the extraction of erroneous spectroscopic factors.

5. CONCLUSIONS

To summarize, we have seen prominent anomalies, attributable to charge exchange, in the (d, p) excitation functions at 168° for at least one of the residual ^{93}Zr states satisfying $Q(d, p) > \frac{1}{4}\Delta_C$ - the $d_{5/2}$ ground state. No significant departure from DWBA predictions is seen for any state of higher excitation. We conclude that the original explanation^{2,7} given for such anomalies is consistent with the $^{92}\text{Zr}(d, p)$ data, and that careful optical and DWBA analysis is capable of a very satisfactory description of (d, p) excitation functions over a fairly broad (7-MeV) energy range, i.e., DWBA spectroscopic factors need not show any energy dependence.

ACKNOWLEDGMENTS

We wish to thank James Kent and James Kulleck for their help in taking the data, and Jim Robertson for his help in reducing the data and preparing the figures. One of us (R.G.C.) gratefully acknowledges the support of an National Defense Education Act (Title IV) fellowship during the past three years. Finally, we appreciate the helpful discussions with C. Fred Moore, and his aid and interest in many phases of this experiment.

†Work supported in part by the U. S. Atomic Energy Commission.

*Present address: Max-Planck Institut für Kernphysik, Heidelberg, Germany.

¹R. G. Clarkson, W. R. Coker, and C. F. Moore, preceding paper [Phys. Rev. C 2, 1097 (1970)]. Fuller references to previous work may be found there.

²C. F. Moore, C. E. Watson, S. A. A. Zaidi, J. J. Kent, and J. G. Kulleck, Phys. Rev. Letters 17, 926 (1966).

³W. R. Coker and C. F. Moore, Phys. Letters 25B, 271 (1967).

⁴C. F. Moore, Phys. Letters 25B, 408 (1967).

⁵R. Heffner, C. Ling, N. Cue, and P. Richard, Phys.

Letters 26B, 150 (1968).

⁶L. S. Michelman and C. F. Moore, Phys. Letters 26B, 446 (1968).

⁷S. A. A. Zaidi and P. von Brentano, Phys. Letters 23B, 466 (1966).

⁸T. Tamura and C. E. Watson, Phys. Letters 25B, 183 (1967).

⁹W. R. Coker and T. Tamura, Phys. Rev. 182, 1277 (1969).

¹⁰R. G. Clarkson, Technical Report No. 3, Center for Nuclear Studies, University of Texas (unpublished); J. G. Page and R. G. Clarkson, Nucl. Instr. Methods 45, 334 (1966).

¹¹R. G. Clarkson and C. E. Watson, unpublished.

¹²J. K. Dickens, E. Eichler, and G. R. Satchler, *Phys. Rev.* **168**, 1355 (1968); J. K. Dickens, E. Eichler, R. J. Silva, and G. Chilosa, Oak Ridge National Laboratory Report No. ORNL-3934, 1966 (unpublished).

¹³W. R. Smith, University of Southern California Report No. USC 136-119, 1967 (unpublished).

¹⁴E. B. Dally, J. B. Nelson, and W. R. Smith, *Phys. Rev.* **152**, 1072 (1966).

¹⁵C. M. Perey and F. G. Perey, *Phys. Rev.* **152**, 923 (1966).

¹⁶P. Kossanyi-Demay and R. de Swiniarski, *Nucl. Phys.* **A104**, 577 (1968).

¹⁷F. G. Perey, *Phys. Rev.* **131**, 745 (1963).

¹⁸Configurations for the states of ^{93}Zr are taken as given

by B. L. Cohen and O. V. Chubinsky, *Phys. Rev.* **131**, 2184 (1963), except for the 3.38-MeV state, here assigned as $l \geq 2$.

¹⁹W. Booth, S. M. Dalgiesh, R. N. Glover, R. F. Hudson, and K. C. McLean, *Phys. Letters* **30B**, 335 (1969).

²⁰J. J. Kent, K. P. Lieb, and C. F. Moore, *Phys. Rev. C* **1**, 337 (1970).

²¹T. Tamura, F. Rybicki, and W. R. Coker, to be published.

²²P. J. A. Buttle and L. J. B. Goldfarb, *Proc. Phys. Soc. (London)* **83**, 701 (1964).

²³M. Lynen, C. V. D. Malsburg, R. Santo, and R. Stock, *Phys. Letters* **24B**, 237 (1967).

Gamma Rays from Thermal and Resonance Neutron Capture in Sb^{121} and Sb^{123} †

M. R. Bhat, R. E. Chrien, D. I. Garber, and O. A. Wasson

Brookhaven National Laboratory, Upton, New York 11973

(Received 27 March 1970)

Prompt high-energy γ rays resulting from neutron capture at thermal energies and in the resonances of Sb^{121} and Sb^{123} have been studied with the high flux beam reactor fast chopper using high-resolution Ge(Li) detectors. The binding energy B_n of the last neutron in Sb^{122} and Sb^{124} has been determined to be 6807 ± 2 and 6468 ± 2 keV, respectively. Based on prompt capture γ -ray data, we have assigned a spin of 4 to the 21.6-eV resonance of Sb^{123} . Energy levels populated by the neutron-capture γ rays are given up to an excitation energy of 2475 keV in Sb^{122} and up to 2221 keV in Sb^{124} . These data are compared with the existing (d, p) data on Sb^{121} and Sb^{123} . We have also studied the low-energy (<511 keV) γ rays originating in neutron capture in the different resonances. For Sb^{121} , the observed spectra are found to fall into two classes, each having its own characteristic intensity distribution depending on the spin of the capturing state. By comparing these spectra with those originating from the 6.24-eV resonance (3^+) and the 15.4-eV resonance (2^+), we have assigned the following spins to the resonances in Sb^{121} : 29.7 eV (3), 53.5 eV (2), 64.5 eV (3), 73.8 eV (2), 111.4 eV (2), and 126.8 eV (3). Similar, but more tentative, spin assignments are made for resonances in Sb^{123} .

The low-energy spectra have also been used to measure the half-life of the 61.6-keV isomeric state in Sb^{122} by a new method. This experimental procedure is described. The half-life of the isomeric state is found to be $2.3 \pm 0.6 \mu\text{sec}$.

1. INTRODUCTION

Antimony is made up of two isotopes, Sb^{121} and Sb^{123} , with fractional abundances of 57.25 and 42.75%, respectively. Neutron capture in these isotopes populates levels in Sb^{122} and Sb^{124} by γ -ray emission. Except for the (d, p) work on Sb^{121} and Sb^{123} by Hjorth,¹ a study^{2,3} of some low-lying levels of Sb^{122} and Sb^{124} , and some recent resonance (n, γ) measurements by Ing *et al.*,⁴ there are no data on the energy levels of Sb^{122} and Sb^{124} . In the (d, p) data mentioned above, the resolution was limited to 40 keV. Also, the zero of the energy scale, and hence the binding energy of the last neutron in these odd-odd nuclei, was not known. Hence, it seemed to be of some interest to study neutron-capture γ rays in antimony. Great interest has been shown in the Sn-Sb region of the periodic ta-

ble, and detailed calculations have been made using the short-range residual interactions to take account of nuclear pairing effects.^{5,6} We hope to supplement the experimental data on nuclei in this region with the present experimental work.

2. EXPERIMENTAL ARRANGEMENT

Neutron-capture γ rays in antimony were studied using the fast chopper at the high-flux beam reactor (HFBR) with a flight path of 21.66 m and a chopper speed of 10 000 rpm. Details of the chopper installation and the on-line data recording and analyzing system have been described before.^{7,8} The chopper was operated at 1500 rpm for recording thermal-neutron-capture events. γ rays originating in resonance capture were recorded with a 10-cc Ge(Li) detector at a resolution of 10 keV at 7.7